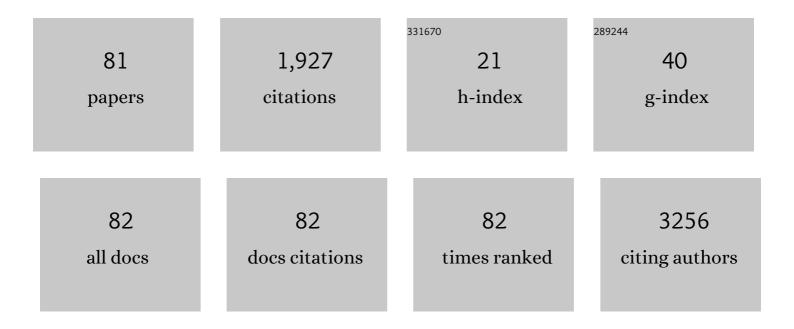
## Mohammed Yaqub Yaqub

List of Publications by Year in descending order

Source: https://exaly.com/author-pdf/831836/publications.pdf Version: 2024-02-01



#	Article	IF	CITATIONS
1	3D Convolutional Neural Network-Based Denoising of Low-Count Whole-Body 18F-Fluorodeoxyglucose and 89Zr-Rituximab PET Scans. Diagnostics, 2022, 12, 596.	2.6	1
2	PET-BIDS, an extension to the brain imaging data structure for positron emission tomography. Scientific Data, 2022, 9, 65.	5.3	20
3	Whole body macrophage PET imaging for disease activity assessment in early rheumatoid arthritis. Journal of Rheumatology, 2022, , jrheum.210928.	2.0	0
4	Impact of cerebral blood flow and amyloid load on SUVR bias. EJNMMI Research, 2022, 12, 29.	2.5	6
5	Longitudinal retinal layer changes in preclinical Alzheimer's disease. Acta Ophthalmologica, 2021, 99, 538-544.	1.1	13
6	What Determines Cognitive Functioning in the Oldest-Old? The EMIF-AD 90+ Study. Journals of Gerontology - Series B Psychological Sciences and Social Sciences, 2021, 76, 1499-1511.	3.9	14
7	Simulating the effect of cerebral blood flow changes on regional quantification of [ <sup>18</sup> F]flutemetamol and [ <sup>18</sup> F]florbetaben studies. Journal of Cerebral Blood Flow and Metabolism, 2021, 41, 579-589.	4.3	12
8	Classification of negative and positive 18F-florbetapir brain PET studies in subjective cognitive decline patients using a convolutional neural network. European Journal of Nuclear Medicine and Molecular Imaging, 2021, 48, 721-728.	6.4	16
9	Effect of Shortening the Scan Duration on Quantitative Accuracy of [18F]Flortaucipir Studies. Molecular Imaging and Biology, 2021, 23, 604-613.	2.6	10
10	Contralateral improvement of cerebrovascular reactivity and TIA frequency after unilateral revascularization surgery in moyamoya vasculopathy. NeuroImage: Clinical, 2021, 30, 102684.	2.7	11
11	Use of population input functions for reduced scan duration whole-body Patlak 18F-FDG PET imaging. EJNMMI Physics, 2021, 8, 11.	2.7	17
12	Onset of Preclinical Alzheimer Disease in Monozygotic Twins. Annals of Neurology, 2021, 89, 987-1000.	5.3	20
13	Test-Retest Variability of Relative Tracer Delivery Rate as Measured by [11C]PiB. Molecular Imaging and Biology, 2021, 23, 335-339.	2.6	2
14	Strategies to reduce sample sizes in Alzheimer's disease primary and secondary prevention trials using longitudinal amyloid PET imaging. Alzheimer's Research and Therapy, 2021, 13, 82.	6.2	14
15	Parametric imaging of dual-time window [18F]flutemetamol and [18F]florbetaben studies. NeuroImage, 2021, 234, 117953.	4.2	7
16	[ <sup>18</sup> F]Flortaucipir PET Across Various <i>MAPT</i> Mutations in Presymptomatic and Symptomatic Carriers. Neurology, 2021, 97, e1017-e1030.	1.1	16
17	Biodistribution of <sup>18</sup> F-FES in patients with metastatic ER+ breast cancer undergoing treatment with Rintodestrant (G1T48), a novel selective estrogen receptor degrader. Journal of Nuclear Medicine, 2021, , jnumed.121.262500.	5.0	2
18	Amyloid-driven disruption of default mode network connectivity in cognitively healthy individuals. Brain Communications, 2021, 3, fcab201.	3.3	14

#	Article	IF	CITATIONS
19	Repeatability of IVIM biomarkers from diffusionâ€weighted MRI in head and neck: Bayesian probability versus neural network. Magnetic Resonance in Medicine, 2021, 85, 3394-3402.	3.0	19
20	Amyloid discordance analysis in cognitively normal monozygotic twins demonstrates that the memory domain is affected first in preclinical AD. Alzheimer's and Dementia, 2021, 17, .	0.8	0
21	Longitudinal [ <sup>18</sup> F]flortaucipir PET: Comparison of quantitative and semiâ€quantitative parameters. Alzheimer's and Dementia, 2021, 17, .	0.8	Ο
22	Optical coherence tomography angiography in preclinical Alzheimer's disease. British Journal of Ophthalmology, 2020, 104, 157-161.	3.9	95
23	Quantitative parametric maps of O-(2-[ <sup>18</sup> F]fluoroethyl)-L-tyrosine kinetics in diffuse glioma. Journal of Cerebral Blood Flow and Metabolism, 2020, 40, 895-903.	4.3	8
24	Parametric methods for [ <sup>18</sup> F]flortaucipir PET. Journal of Cerebral Blood Flow and Metabolism, 2020, 40, 365-373.	4.3	22
25	Associations of Brain Pathology Cognitive and Physical Markers With Age in Cognitively Normal Individuals Aged 60–102 Years. Journals of Gerontology - Series A Biological Sciences and Medical Sciences, 2020, 75, 1609-1617.	3.6	7
26	Multitracer model for staging cortical amyloid deposition using PET imaging. Neurology, 2020, 95, e1538-e1553.	1.1	55
27	CSF proteomic changes in preâ€preclinical Alzheimer's disease: A monozygotic twin study. Alzheimer's and Dementia, 2020, 16, e038966.	0.8	0
28	Amyloidâ€Î² deposition in cognitively normal oldestâ€old is associated with cortical thinning and faster memory decline. Alzheimer's and Dementia, 2020, 16, e040991.	0.8	0
29	Amyloidâ€Î² deposition in cognitively normal oldestâ€old is associated with cortical thinning and faster memory decline. Alzheimer's and Dementia, 2020, 16, e042768.	0.8	Ο
30	Amyloid aggregation and subsequent memory decline over time in cognitively intact older identical twins. Alzheimer's and Dementia, 2020, 16, e045112.	0.8	0
31	Quantitative accuracy remains after shortening of dynamic [ 18 F]flortaucipir PET protocol. Alzheimer's and Dementia, 2020, 16, e045710.	0.8	0
32	11C-sorafenib and 15O-H2O PET for early evaluation of sorafenib therapy. Journal of Nuclear Medicine, 2020, 62, jnumed.120.251611.	5.0	0
33	Diagnostic Value of Magnetic Resonance Imaging in Fibrodysplasia Ossificans Progressiva. JBMR Plus, 2020, 4, e10363.	2.7	7
34	First in man study of [18F]fluoro-PEG-folate PET: a novel macrophage imaging technique to visualize rheumatoid arthritis. Scientific Reports, 2020, 10, 1047.	3.3	43
35	Repeatability of arterial input functions and kinetic parameters in muscle obtained by dynamic contrast enhanced MR imaging of the head and neck. Magnetic Resonance Imaging, 2020, 68, 1-8.	1.8	19
36	[11C]PIB amyloid quantification: effect of reference region selection. EJNMMI Research, 2020, 10, 123.	2.5	17

#	Article	IF	CITATIONS
37	Optimized dual-time-window protocols for quantitative [18F]flutemetamol and [18F]florbetaben PET studies. EJNMMI Research, 2019, 9, 32.	2.5	31
38	Direct comparison of [11C] choline and [18F] FET PET to detect glioma infiltration: a diagnostic accuracy study in eight patients. EJNMMI Research, 2019, 9, 57.	2.5	8
39	Amyloid imaging of dutchâ€ŧype hereditary cerebral amyloid angiopathy carriers. Annals of Neurology, 2019, 86, 616-625.	5.3	22
40	Applying the ATN scheme in a memory clinic population. Neurology, 2019, 93, e1635-e1646.	1.1	51
41	Assessment of the appropriate use criteria for amyloid PET in an unselected memory clinic cohort: The ABIDE project. Alzheimer's and Dementia, 2019, 15, 1458-1467.	0.8	18
42	Exploring effects of Souvenaid on cerebral glucose metabolism in Alzheimer's disease. Alzheimer's and Dementia: Translational Research and Clinical Interventions, 2019, 5, 492-500.	3.7	5
43	Amyloid-β Load Is Related to Worries, but Not to Severity of Cognitive Complaints in Individuals With Subjective Cognitive Decline: The SCIENCe Project. Frontiers in Aging Neuroscience, 2019, 11, 7.	3.4	37
44	Retinal layer thickness in preclinical Alzheimer's disease. Acta Ophthalmologica, 2019, 97, 798-804.	1.1	36
45	Evolution of heterotopic bone in fibrodysplasia ossificans progressiva: An [18F]NaF PET/CT study. Bone, 2019, 124, 1-6.	2.9	20
46	Assessment of Simplified Methods for Quantification of 18F-FDHT Uptake in Patients with Metastatic Castration-Resistant Prostate Cancer. Journal of Nuclear Medicine, 2019, 60, 1221-1227.	5.0	10
47	Association of amyloid pathology with memory performance and cognitive complaints in cognitively normal older adults: a monozygotic twin study. Neurobiology of Aging, 2019, 77, 58-65.	3.1	14
48	Evaluation of the Novel PET Tracer [11C]HACH242 for Imaging the GluN2B NMDA Receptor in Non-Human Primates. Molecular Imaging and Biology, 2019, 21, 676-685.	2.6	8
49	Semi-quantitative cerebral blood flow parameters derived from non-invasive [ <sup>15</sup> 0]H <sub>2</sub> 0 PET studies. Journal of Cerebral Blood Flow and Metabolism, 2019, 39, 163-172.	4.3	12
50	Feasibility of state of the art PET/CT systems performance harmonisation. European Journal of Nuclear Medicine and Molecular Imaging, 2018, 45, 1344-1361.	6.4	100
51	Molecular Imaging of ABCB1 and ABCG2 Inhibition at the Human Blood–Brain Barrier Using Elacridar and <sup>11</sup> C-Erlotinib PET. Journal of Nuclear Medicine, 2018, 59, 973-979.	5.0	19
52	Effects of intravenous thyrotropin-releasing hormone on 18F-fluorodeoxyglucose uptake in human brown adipose tissue: a randomized controlled trial. European Journal of Endocrinology, 2018, 179, 31-38.	3.7	15
53	Quantification of O-(2-[18F]fluoroethyl)-L-tyrosine kinetics in glioma. EJNMMI Research, 2018, 8, 72.	2.5	14
54	A novel partial volume correction method for accurate quantification of [18F] flortaucipir in the hippocampus. EJNMMI Research, 2018, 8, 79.	2.5	19

#	Article	IF	CITATIONS
55	Resilience to cognitive impairment in the oldest-old: design of the EMIF-AD 90+ study. BMC Geriatrics, 2018, 18, 289.	2.7	25
56	The EMIF-AD PreclinAD study: study design and baseline cohort overview. Alzheimer's Research and Therapy, 2018, 10, 75.	6.2	48
57	Hypometabolism of the posterior cingulate cortex is not restricted to Alzheimer's disease. NeuroImage: Clinical, 2018, 19, 625-632.	2.7	23
58	Association of Amyloid Positron Emission Tomography With Changes in Diagnosis and Patient Treatment in an Unselected Memory Clinic Cohort. JAMA Neurology, 2018, 75, 1062.	9.0	102
59	Quantification of Tau Load Using [18F]AV1451 PET. Molecular Imaging and Biology, 2017, 19, 963-971.	2.6	42
60	Impact of <scp>PET</scp> / <scp>CT</scp> system, reconstruction protocol, data analysis method, and repositioning on <scp>PET</scp> / <scp>CT</scp> precision: An experimental evaluation using an oncology and brain phantom. Medical Physics, 2017, 44, 6413-6424.	3.0	30
61	Parametric Methods for Dynamic 11C-Phenytoin PET Studies. Journal of Nuclear Medicine, 2017, 58, 479-483.	5.0	2
62	Model selection criteria for dynamic brain PET studies. EJNMMI Physics, 2017, 4, 30.	2.7	18
63	Investigation of practical initial attenuation image estimates in TOFâ€MLAA reconstruction for PET/MR. Medical Physics, 2016, 43, 4163-4173.	3.0	11
64	In vivo (R)-[11C]PK11195 PET imaging of 18kDa translocator protein in recent onset psychosis. NPJ Schizophrenia, 2016, 2, 16031.	3.6	63
65	Effects of erlotinib therapy on [11C]erlotinib uptake in EGFR mutated, advanced NSCLC. EJNMMI Research, 2016, 6, 10.	2.5	30
66	Investigating the state-of-the-art in whole-body MR-based attenuation correction: an intra-individual, inter-system, inventory study on three clinical PET/MR systems. Magnetic Resonance Materials in Physics, Biology, and Medicine, 2016, 29, 75-87.	2.0	62
67	Quantitative and Simplified Analysis of <sup>11</sup> C-Erlotinib Studies. Journal of Nuclear Medicine, 2016, 57, 861-866.	5.0	22
68	Evaluation of the accuracy of the average Mu-values within patients from MR derived Mu-maps. , 2015, ,		0
69	Effects of boundary conditions in TOF-MLAA reconstruction for PET/MR. , 2015, , .		0
70	Evaluation of a more optimal initial attenuation image estimate in TOF-MLAA for PET/MR. , 2015, , .		0
71	Detecting resistance in EGFR-mutated non-small-cell lung cancer after clonal selection through targeted therapy. Personalized Medicine, 2015, 12, 63-66.	1.5	1
72	A Clinical and Experimental Comparison of Time of Flight PET/MRI and PET/CT Systems. Molecular Imaging and Biology, 2015, 17, 714-725.	2.6	10

#	Article	IF	CITATIONS
73	The Dopamine Stabilizer (â^')-OSU6162 Occupies a Subpopulation of Striatal Dopamine D2/D3 Receptors: An [11C]Raclopride PET Study in Healthy Human Subjects. Neuropsychopharmacology, 2015, 40, 472-479.	5.4	22
74	Quantification of Dynamic <sup>11</sup> C-Phenytoin PET Studies. Journal of Nuclear Medicine, 2015, 56, 1372-1377.	5.0	17
75	Parametric Methods for Quantification of 18F-FAZA Kinetics in Non–Small Cell Lung Cancer Patients. Journal of Nuclear Medicine, 2014, 55, 1772-1777.	5.0	12
76	Assessment of Simplified Methods to Measure <sup>18</sup> F-FLT Uptake Changes in EGFR-Mutated Non–Small Cell Lung Cancer Patients Undergoing EGFR Tyrosine Kinase Inhibitor Treatment. Journal of Nuclear Medicine, 2014, 55, 1417-1423.	5.0	17
77	Longitudinal Amyloid Imaging Using <sup>11</sup> C-PiB: Methodologic Considerations. Journal of Nuclear Medicine, 2013, 54, 1570-1576.	5.0	148
78	Optimization of Supervised Cluster Analysis for Extracting Reference Tissue Input Curves in ( <i>R</i> )-[ <sup>11</sup> C]PK11195 Brain PET Studies. Journal of Cerebral Blood Flow and Metabolism, 2012, 32, 1600-1608.	4.3	120
79	Simplified parametric methods for [11C]PIB studies. NeuroImage, 2008, 42, 76-86.	4.2	85
80	Optimization algorithms and weighting factors for analysis of dynamic PET studies. Physics in Medicine and Biology, 2006, 51, 4217-4232.	3.0	81
81	Improving accuracy and precision of PET pharmacokinetic analysis using wavelet based denoising of time activity curves. Journal of Cerebral Blood Flow and Metabolism, 2005, 25, S640-S640.	4.3	1